Soil thawing regulates the spring growth onset in tundra and alpine biomes

Adrià Descals, Aleixandre Verger, Iolanda Filella, Dennis Baldocchi, Ivan A Janssens, Yongshuo H Fu, Shilong Piao, Marc Peaucelle, Philippe Ciais, Josep Peñuelas

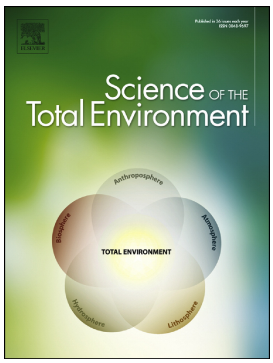

Soil thawing regulates the spring growth onset in tundra and alpine biomes

Adrià Descals, Aleixandre Verger, Iolanda Filella, Dennis Baldocchi, Ivan A. Janssens, Yongshuo H. Fu, Shilong Piao, Marc Peaucelle, Philippe Ciais, Josep Peñuelas

PII: S0048-9697(20)34159-0

DOI: https://doi.org/10.1016/j.scitotenv.2020.140637

Reference: STOTEN 140637

To appear in: *Science of the Total Environment*

Received date: 28 April 2020

Revised date: 25 June 2020

Accepted date: 28 June 2020

Please cite this article as: A. Descals, A. Verger, I. Filella, et al., Soil thawing regulates the spring growth onset in tundra and alpine biomes, *Science of the Total Environment* (2020), https://doi.org/10.1016/j.scitotenv.2020.140637

TITLE: Soil thawing regulates the spring growth onset in tundra and alpine biomes

Adrià Descals[1,2], Aleixandre Verger[1,2], Iolanda Filella[1,2], Dennis Baldocchi[3], Ivan A. Janssens[4], Yongshuo H. Fu[5], Shilong Piao[6], Marc Peaucelle[1,2], Philippe Ciais[7] & Josep Peñuelas[1,2]

1 CREAF, Cerdanyola del Vallès, Barcelona 08193, Catalonia, Spain
2 CSIC, Global Ecology Unit CREAF-CSIC-UAB, Bellaterra, Barcelona 08193, Catalonia, Spain
3 University of California, Berkeley, United States.
4 Department of Biology, University of Antwerp, Wilrijk, 2610, Belgium
5 College of Water Sciences, Beijing Normal University, Beijing, China
6 Peking University, China
7 LSCE, Gif-sur-Yvette, France

e-mail addresses: a.descals@creaf.uab.cat, verger@creaf.uab.cat, iola@creaf.uab.cat, baldocchi@berkeley.edu, ivan.janssens@uantwerpen.be, yongshuo.fu@uantwerpen.be, slpiao@pku.edu.cn, mpeau.pro@gmail.com, philippe.ciais@lsce.ipsl.fr, Josep.Penuelas@uab.cat

Corresponding author: Adrià Descals, a.descals@creaf.uab.cat +34 680 71 97 24

TITLE: Soil thawing regulates the spring growth onset in tundra and alpine biomes

Abstract

Soil temperature remains isothermal at 0 °C and water shifts to a liquid phase during soil thawing. Vegetation may receive this process as a signal and a key to restore physiological activity. We aimed to show the relationship between the timing of soil thawing and the spring growth onset. We estimated the delay between the soil thawing and the spring growth onset in 78 sites of the FLUXNET network. We built a soil thawing map derived from modelling for the northern hemisphere and related it to the greenness onset estimated with satellite imagery. Spring onset estimated with GPP time series occurred shortly after soil surface thawing in tundra (1.1 ± 3.5 days) and alpine grasslands (16.6 ± 5.8 days). The association was weaker for deciduous forests (40.3 ± 4.2 days), especially where soils freeze infrequently. Needleaved forests tended to start the growing season before the end of thawing (-17.4 ± 3.6 days), although observations from remote sensing (MODIS Land Cover Dynamics) indicated that the onset of greenness started after the thawing period (26.8 ± 3.2 days). This study highlights the role of soil temperature at the spring growth onset at high latitudes. Soil thawing becomes less relevant in temperate forests, where soil is occasionally frozen and other climate factors become more important.

Keywords: Boreal forests, deciduous forests, plant phenology, spring onset, thawing, tundra.

1. Introduction

Phenology is defined as the timing of periodic life-cycle events (Schwartz, 2003). Phenology has recently gained attention as an indicator of global warming and more broadly for its link with global environmental change (Badeck et al., 2004; Cleland et al., 2007; Peñuelas et al., 2009; Peñuelas & Filella, 2001). Plant phenology is primarily modulated by the seasonal variation in climate, which involves a stage of dormancy when the climate is adverse and a period of growth when conditions are favorable for vegetation activity. Temperature, water availability, and day length have been proposed as the main environmental drivers that constrain vegetation activity and regulate plant phenology, acting eventually as confounded restraints for vegetation growth (Chuine & Régnière, 2017; Jolly et al., 2005; Kramer & Hänninen, 2009). Temperature is the main climatic factor regulating plant phenology for the onset of vegetation in the northern high latitudes (Schwartz, 2003). Evidence for the interaction of temperature with other limiting factors, e.g. photoperiod and water availability, though, is under discussion (Fu et al., 2019; Körner & Basler, 2010; Peñuelas et al., 2004) and, the choice of the climatic variables for modeling phenology is an open science question.

Air temperature has been widely used to simulate the transition from dormancy to growth in temperature-limited biomes, and jointly with day length, an indicator of photoperiod, for modeling plant phenology in the Northern Hemisphere (Badeck et al., 2004; Peñuelas & Filella, 2001). Some biome-specific studies, however, have suggested that soil temperature more accurately indicates the start of the growing season (Baldocchi et al., 2005; Jiang et al., 2018; Lieth, 2013; Semenchuk et al., 2016; Starr et al., 2008), although a study showed a stronger connection with air temperature than soil temperature for boreal forests (Tanja et al., 2003). Some studies even suggested that the lengthening of the growing season in tundra during recent decades was primarily caused by a change in the seasonal thaw cycle (Barichivich et al., 2013;

Kimball et al., 2006). A soil warming experiment in subarctic grasslands, which reduced the occurrence of soil frost, revealed that the growing season lengthened across the entire range of IPCC warming projections for 2100 and reported no indications of photoperiod constraints within that warming range (Leblans et al., 2017).

A frozen soil strictly limits vegetation growth and overrules any impact of eventual favorable air temperatures during spring. Thawing occurs when soil remains isothermal at 0 °C, triggering some processes that may be used as signals for the vegetation to restore physiological activity. Water only returns to its liquid form and becomes available to roots (Noormets, 2009) during and after thawing. In addition to a direct signal of soil thawing, soil temperature has been found to exert a stronger influence on plants than air temperature. For example, soil temperature has also been associated with physiological processes such as root elongation (Wang et al., 2018) and root respiration (Lloyd & Taylor, 1994). Soil warming experiments have found that an overall increase in soil temperature affected specific traits; leaf area, leaf expansion rates, and diameter growth in deciduous trees (Farnsworth et al., 1995; Wheeler et al., 2016), needle starch content and photochemical efficiency in boreal forests (Repo et al., 2004), and flowering frequency in tundra (Khorsand et al., 2015).

These results suggest that soil temperature may play a more deterministic limiting role than air temperature at the onset of spring at high latitudes. We tested the hypothesis that soil thawing regulates spring growth onset at high latitudes but becomes less relevant where soil is only sporadically frozen.

2. Materials and Methods

2.1. Phenology derived from in situ and satellite data

We used the same methodology as Zhang *et al*, 2003 to estimate the start of season at the FLUXNET sites. We took the daily mean gross primary productivity (GPP) measurements (daytime partitioning method) and adjusted a logistic function for each year for the period January 1st to July 1st. The start of season at the FLUXNET sites (GPP SoS) was the day when the second derivative of the logistic function was maximal.

We used the MCD12Q2 V5 Land Cover Dynamics product (MODIS SoS) for the period 2001-2014. MCD12Q2 phenological metrics are estimated yearly, with a logistic function fitted over the MODIS EVI time series (Zhang et al., 2003). We used the layer 'Onset Greenness Increase', which represents the day of the year on which the positive curvature of the fitted logistic function is maximal.

2.2. Estimation of the start and end of thawing

We defined the end of thawing (EoT) as the last day before solstice with daily mean soil temperature <0.5 °C and defined the start of thawing (SoT) as the closest day before EoT with a temperature below -0.5 °C. We estimated the EoT and SoT using the *in situ* records of soil temperature at the FLUXNET sites in the Profile 1 (TS_1_1_1), which corresponds to soil temperature measured at the shallowest layer, with a different depth depending on the FLUXNET site but commonly 2-5 centimeters. The EoT was also estimated using the layer of soil temperature at 10-centimeter depth available in the Global Land Data Assimilation System (GLDAS) dataset (See section 2.3.). This resulted in global maps of EoT at 0.25° resolution. We used a threshold of 0.5 °C instead of 0 °C to avoid false-positive estimates of EoT due to noise and slight variations in the soil temperature time series during thawing.

2.3. Global climatic data set

We used the GLDAS version 2.1 as a global climatic data set for the daily representation of soil temperature at a global scale. GLDAS is a land-surface modeling system developed by the Goddard Space Flight Center of the National Aeronautics and Space Administration and by the National Centers for Environmental Prediction of the National Oceanic and Atmospheric Administration. The version 2.1 provides data for the period 2000 up until the present time. Ground measurements (meteorological data), such as soil temperature, and satellite observations are ingested in order to constrain the land-surface model and constrain unrealistic model states. GLDAS offers 3-hourly estimates of earth-surface variables such as soil temperature at different depths. We used the soil temperature product at 10-centimeter depth with a spatial resolution of 0.25°.

2.4. Resizing and filtering MODIS SoS

The spatial resolutions of GLDAS EoT and MODIS SoS differed, so we resized the resolution of MODIS SoS (500 m) to the resolution of GLDAS EoT (0.25°) to make the comparison between the two datasets consistent. We first masked the yearly MODIS SoS images with the MODIS IGBP Land Cover (MCD12Q1) product. MODIS SoS was masked separately with the IGBP classes 1) deciduous broadleaved forests (deciduous forests), 2) evergreen needleleaved forests (needleleaved forests), 3) shrubland, 4) open shrubland, and 5) grassland. For the tundra biome, we only considered the pixels classified as shrubland, open shrubland, and grassland at >50° latitude. Finally, the masked MODIS SoS images were resized to 0.25° using the mean as the resampling operation. This resulted in six sets of MODIS SoS for each land cover for the period 2001-2014.

2.5. Experimental setup and statistical analyses

We analyzed 78 sites of the FLUXNET network and compared the timing of spring onset of ecosystem GPP with thawing date. We used all sites north of 30°N latitude that are located in tundra (13 sites) and alpine (4 sites) climates, and the sites categorized in the IGBP classification as deciduous broadleaved forests (DBF) (18 sites in temperate and 1 site boreal climate zones) or evergreen needleaved forests (ENF) (25 sites in temperate and 17 sites boreal climate zones). Table S1 shows the coordinates and biome of the selected sites. We excluded the sites without in situ soil temperature records.

We investigated at which soil temperature the GPP was significantly positive in each biome. We grouped the half-hourly GPP observations in intervals of 0.5°C of soil temperature. We applied a two-tailed Student's t-test at each interval of soil temperature with a significance of 95%. We considered that GPP was positive at a certain temperature when the lower GPP confidence interval was greater than 0.5 μmol CO_2 m^{-2} s^{-1}.

The SoT and EoT estimated with the FLUXNET records were compared with two independent observations of the start of the growing season (SoS): 1) SoS estimated with daily *in situ* observations of the FLUXNET GPP time series (GPP SoS) and 2) SoS extracted from remote-sensing sources (MODIS SoS). We applied the two-tailed Student's t-test with a significance of 95% to find whether the day of the EoT and the spring onset (GPP SoS and MODIS SoS) were significantly different. We reported the mean difference, confidence interval, and coefficient of determination (R^2) between the end of thawing and the spring onset.

We also compared the spring onset observed with satellite derived data (MODIS SoS) with the thawing period estimated with the GLDAS. The MODIS SoS was filtered and resized to the

resolution of the GLDAS to make the datasets comparable. Similarly to the comparison at the FLUXNET sites, we reported the R^2 and the mean difference with a confidence interval of 95% between the EoT and the MODIS SoS. The analysis covers a time period from 2000 to 2015 for the comparison between FLUXNET and MODIS, and from 2001 to 2017 for the comparison between the GLDAS and MODIS.

3. Results

The growing seasons were primarily driven by temperature in the 73 FLUXNET sites; GPP and air temperature had similar intra-seasonal patterns. Gross primary productivity at these sites was highest in summer, when the air and soil temperatures were also highest. The Italian site IT-Ro1 was the only exception, where GPP decreased during summer due to water stress. A representation of air and soil temperature, GPP and spring onset is shown in Fig. S1 for five FLUXNET sites. GPP was insignificant with frozen soil in all biomes (Fig. 1). The lowest soil temperature at which GPP was significantly higher than 0.5 μmol CO_2 m^{-2} s^{-1} was 1°C in tundra, -0.5°C in alpine grasslands, -1 °C in needleaved forests, and 4.5 °C in deciduous forests.

Spring onset occurred during thawing (41% of observations for GPP SoS and 6% of the observations for MODIS SoS) or after EoT (51% of observations for GPP SoS and 59% of the observations for MODIS SoS) (Fig. 2). Only 8% of the observations occurred when soil was frozen in GPP SoS, primarily in needleaved forests. Spring onset for tundra and alpine grasslands tended to start shortly after the EoT (1.1 ± 3.5 d for GPP SoS and 18.5 ± 3.0 d for MODIS SoS for tundra, 16.6 ± 5.8 d for GPP SoS and 32.9 ± 8.3 d for MODIS SoS for alpine grasslands). Spring onset tended to start with a longer delay after EoT in deciduous forests with seasonally frozen soil (40.3 ± 4.2 d for GPP SoS and 46.4 ± 3.8 d for MODIS SoS), while needleleaved

forests showed discrepant results between the two sources of data (-17.3 ± 3.6 d for GPP SoS and 26.8 ± 3.2 d for MODIS SoS).

The association between the GPP SoS and the EoT SoS is different in deciduous than in needleleaved forests (Fig. 3a). Spring onset occurs with positive temperatures in deciduous forests, while needleleaved forest starts their growing season before the soil has completely thawed. Tundra and alpine grasslands show the highest agreement of spring onset with the EoT (*RMSE* = 9.03 in GPP SoS and *RMSE* = 20.45 in MODIS SoS). FLUXNET sites in the boreal biome also showed a better agreement than the sites in the temperate biome in both GPP SoS and MODIS SoS (Fig. S2). In addition, soil did not freeze in some sites of the temperate biome, which explains the EoT values equal to 0 in Fig. 3 and Fig. S2.

The comparison of MODIS SoS with the global estimates of EoT (Fig. 4) led to similar results as the observations at the FLUXNET sites. The onset of greenness estimated with MODIS occurred near EoT in the land cover types that represent tundra (8.63 ± 7.96 d in shrubland IGBP class, 16.97 ± 7.72 d in open shrubland IGBP class, and 18.80 ± 14.55 d in grassland IGBP class), while deciduous forests showed the highest delay (34.24 ± 18.59 d). The high delay in deciduous forests can be observed in the map showing the difference mean MODIS SoS - mean EoT (Fig. 5) at the most southerly latitudes of the deciduous forest distribution (eastern North America, central Europe, and northern China). We observed a high interannual variability in the MODIS SoS and EoT also at low latitudes (Fig. S3). Contrarily to the results in the FLUXNET sites, the MODIS SoS in needleleaved forests show a similar pattern as deciduous forests and do not present a negative delay compared to the EoT (20.03 ± 14.15 d).

4. Discussion

Spring onset of vegetation activity and soil thawing were closely associated in tundra and alpine grasslands, and weakly associated where soil froze intermittently. Water remains inaccessible to plants in frozen soils, inhibiting vegetation activity. This process is particularly relevant in regions with deep frost, where the vegetation has maximal root depth <0.5 m in tundra or <2 m in boreal forests (Canadell et al., 1996). Likewise, most root biomass in boreal and temperate forests is in shallow soil layers, where most mineralization processes release the greatest amount of nutrients. Frozen soil, even if only the first few centimeters, may therefore imply inhibition of vegetation activity, as suggested by the results from the FLUXNET towers, where the GPP is insignificant when soil temperatures are negative (Fig. 1). In addition, most of the observations of spring onset, both MODIS SoS and GPP SoS, coincided with positive or near freezing soil temperatures (Fig. 2).

Water gradually shifts from the solid to the liquid form during thawing, which plants may use as a signal to start their activity. Our results, however, indicated that the time between EoT and spring onset depended on the biome. These differences can be attributed to different forcing requirements for which vegetation has different adaptive histories. Deciduous forests seem to require greater heat accumulation than tundra and needleleaved forests to initiate spring growth. Many studies have suggested that the high thermal forcing required by deciduous trees, which delays the vegetation onset date after the EoT, is an adaptation to prevent frost damage in late spring (Fu et al., 2015; Laube et al., 2014). In addition, deciduous forests have adapted their high thermal forcing depending on the background climate (Peaucelle et al., 2019), with lower heat requirements in colder climates. This would explain the high delay between the spring onset and EoT in deciduous forest in the lowest latitudes of the study, while the only FLUXNET site with deciduous forests located in the boreal zone shows a close association between the spring onset

and the thawing period. Similarly to the site with deciduous forest in the boreal biome, tundra and alpine grasslands have a low heat requirements, very likely because their SoS also occurs very late in the season, when light availability is already high, and these plants may therefore have reduced their heat requirement to maximize profit from the high light conditions in late spring.

Our results show that needleaved forests can release from dormancy and start their gross primary production during the thawing period with near freezing soil temperatures, which corroborates the photosynthetic acclimation to cold in boreal needleaved forests (Oquist & Huner, 2003). However, the results obtained from remote sensing show that the onset in greenness in needleaved forests occurs much closer to the end of the thawing period. This suggests that evergreen needleaved trees start the growing season when temperatures become favorable using the needles preserved during the dormant period, but needle emergence occurs much later than the start of the photosynthetic activity. The delay between GPP SoS and onset of greenness was also observed with remotely-sensed data in previous studies (Melaas et al., 2013; Walther et al., 2016). An alternative explanation for the early GPP SoS in boreal forests is that understory might have started the photosynthetic activity before the trees in the overstory and, thus, vegetation in the understory layer accounted for the carbon fluxes before the thawing period. This would be supported by the findings of Ikawa et al., 2015, which showed the contributions of the understory in boreal ecosystems to the carbon and energy balances.

The hypothesis that tundra has adapted to the long period with frozen soils by reducing its heat requirement implies that spring onset is highly responsive to soil thawing. This hypothesis is supported by studies with long time series of snow melt and by soil-warming experiments reporting that spring onset is advanced by an increasingly earlier soil thawing (Barichivich et al.,

2013; Kimball et al., 2006; Leblans et al., 2017). Spring onset in arctic and subarctic vegetation may thus continue to advance as soil thawing occurs earlier with climate warming. The possible restriction in vegetation growth because of insufficient levels of incoming radiation or hours of sunshine is, however, still undetermined.

Our results suggest that the role of soil temperature is secondary at southerly latitudes for deciduous and needleaved forests. Sites with favorable soil and air temperatures throughout the year may be constrained by photoperiod (Zohner et al., 2016), by chilling requirements (Chuine et al., 2010), or by both (Fu et al., 2019). These regions without soil temperature regulation had the largest differences between MODIS SoS and EoT, as observed in the difference map in Figure 5. The differences observed between the EoT and the GPP SoS at the FLUXNET towers with needleleaved forests cannot be depicted with the MODIS SoS and, thus, are not reflected in the map in Figure 5.

In summary, we demonstrate that spring onset rarely occurs with negative soil temperatures, indicating that frozen soil acted as a major constraint on vegetation activity. We also demonstrate that vegetation activity began shortly after thawing in tundra, after soil temperatures at 2-centimeter depth surpassed the 0 °C threshold. This correlation became weaker for lower latitudes. Needleleaved forests can start the gross primary production during the thawing period, while deciduous forests delayed the spring onset especially at more southerly latitudes. These results thus provide insight in the onset of spring that can be used for improving phenological models, especially in tundra and boreal forests where soil thawing plays a major role in controlling the start of vegetation activity. Further studies may take advantage of recent advances in mapping soil thawing using microwave remote sensing to estimate the start of the growing season at northern latitudes.

Data availability statement

The data that support the findings of the study are openly available from FLUXNET at [https://fluxnet.fluxdata.org/], GLDAS version 2.1 at [https://ldas.gsfc.nasa.gov/gldas/], MODIS Land Cover Type MMCD12Q1v6 at [https://doi.org/10.5067/MODIS/MCD12Q1.006], and MODIS Land Cover Dynamics MCD12Q2v6 at [https://doi.org/10.5067/MODIS/MCD12Q2.006].

Code availability

The code is available from the authors upon request.

Acknowledgements

The authors would like to acknowledge the financial support from the European Research Council Synergy grant ERC-SyG-2013-610028 IMBALANCE-P, the Spanish Government grant PID2019-110521GB-I00 and the Catalan Government grant SGR 2017-1005.

References

Badeck, F., Bondeau, A., Böttcher, K., Doktor, D., Lucht, W., Schaber, J., & Sitch, S. (2004). Responses of spring phenology to climate change. *New Phytologist*, *162*(2), 295–309.

Baldocchi, D. D., Black, T. A., Curtis, P. S., Falge, E., Fuentes, J. D., Granier, A., Gu, L., Knohl, A., Pilegaard, K., Schmid, H. P., Valentini, R., Wilson, K., Wofsy, S., Xu, L., & Yamamoto, S. (2005). Predicting the onset of net carbon uptake by deciduous forests with soil temperature and climate data: A synthesis of FLUXNET data. *International Journal of Biometeorology*, *49*(6), 377–387. https://doi.org/10.1007/s00484-005-0256-4

Barichivich, J., Briffa, K. R., Myneni, R. B., Osborn, T. J., Melvin, T. M., Ciais, P., Piao, S., & Tucker, C. (2013). Large-scale variations in the vegetation growing season and annual cycle of atmospheric

CO2 at high northern latitudes from 1950 to 2011. *Global Change Biology*, *19*(10), 3167–3183. https://doi.org/10.1111/gcb.12283

Canadell, J., Jackson, R., Ehleringer, J., Mooney, H., Sala, O., & Schulze, E.-D. (1996). Maximum rooting depth of vegetation types at the global scale. *Oecologia*, *108*(4), 583–595.

Chuine, I., Morin, X., & Bugmann, H. (2010). Warming, Photoperiods, and Tree Phenology. *Science*, *329*(5989), 277–278. https://doi.org/10.1126/science.329.5989.277-e

Chuine, I., & Régnière, J. (2017). Process-Based Models of Phenology for Plants and Animals. *Annual Review of Ecology, Evolution, and Systematics*, *48*(1), 159–182. https://doi.org/10.1146/annurev-ecolsys-110316-022706

Cleland, E. E., Chuine, I., Menzel, A., Mooney, H. A., & Schwartz, M. D. (2007). Shifting plant phenology in response to global change. *Trends in Ecology & Evolution*, *22*(7), 357–365. https://doi.org/10.1016/j.tree.2007.04.003

Farnsworth, E. J., Nunez-Farfan, J., Careaga, S. A., & Bazzaz, F. A. (1995). Phenology and Growth of Three Temperate Forest Life Forms in Response to Artificial Soil Warming. *Journal of Ecology*, *83*(6), 967–977. https://doi.org/10.2307/2261178

Fu, Y. H., Zhang, X., Piao, S., Hao, F., Geng, X., Vitasse, Y., Zohner, C., Peñuelas, J., & Janssens, I. A. (2019). Daylength helps temperate deciduous trees to leaf-out at the optimal time. *Global Change Biology*, *0*. https://doi.org/10.1111/gcb.14633

Fu, Y. H., Zhao, H., Piao, S., Peaucelle, M., Peng, S., Zhou, G., Ciais, P., Huang, M., Menzel, A., Peñuelas, J., Song, Y., Vitasse, Y., Zeng, Z., & Janssens, I. A. (2015). Declining global warming effects on the phenology of spring leaf unfolding. *Nature*, *526*(7571), 104–107. https://doi.org/10.1038/nature15402

Ikawa, H., Nakai, T., Busey, R. C., Kim, Y., Kobayashi, H., Nagai, S., Ueyama, M., Saito, K., Nagano, H., Suzuki, R., & others. (2015). Understory CO2, sensible heat, and latent heat fluxes in a black spruce forest in interior Alaska. *Agricultural and Forest Meteorology*, *214*, 80–90.

Jiang, H., Zhang, W., Yi, Y., Yang, K., Li, G., & Wang, G. (2018). The impacts of soil freeze/thaw dynamics on soil water transfer and spring phenology in the Tibetan Plateau. *Arctic, Antarctic, and Alpine Research*, *50*(1), e1439155. https://doi.org/10.1080/15230430.2018.1439155

Jolly, W. M., Nemani, R., & Running, S. W. (2005). A generalized, bioclimatic index to predict foliar phenology in response to climate. *Global Change Biology*, *11*(4), 619–632. https://doi.org/10.1111/j.1365-2486.2005.00930.x

Khorsand, R., Oberbauer, S., Starr, G., La Puma, I., Pop, E., Arquist, L., & Baldwin, T. (2015). Plant phenological responses to a long-term experimental extension of growing season and soil warming in the tussock tundra of Alaska. *Global Change Biology*, *21*. https://doi.org/10.1111/gcb.13040

Kimball, J. S., McDonald, K. C., & Zhao, M. (2006). Spring Thaw and Its Effect on Terrestrial Vegetation Productivity in the Western Arctic Observed from Satellite Microwave and Optical Remote Sensing. *Earth Interactions*, *10*(21), 1–22. https://doi.org/10.1175/EI187.1

Körner, C., & Basler, D. (2010). Phenology Under Global Warming. *Science*, *327*(5972), 1461–1462. https://doi.org/10.1126/science.1186473

Kramer, K., & Hänninen, H. (2009). The Annual Cycle of Development of Trees and Process-Based Modelling of Growth to Scale Up From the Tree To the Stand. In A. Noormets (Ed.), *Phenology of Ecosystem Processes: Applications in Global Change Research* (pp. 201–227). Springer New York. https://doi.org/10.1007/978-1-4419-0026-5_9

Laube, J., Sparks, T. H., Estrella, N., Höfler, J., Ankerst, D. P., & Menzel, A. (2014). Chilling outweighs photoperiod in preventing precocious spring development. *Global Change Biology*, *20*(1), 170–182.

Leblans, N. I. W., Sigurdsson, B. D., Vicca, S., Fu, Y., Penuelas, J., & Janssens, I. A. (2017). Phenological responses of Icelandic subarctic grasslands to short-term and long-term natural soil warming. *Global Change Biology*, *23*(11), 4932–4945. https://doi.org/10.1111/gcb.13749

Lieth, H. (2013). *Phenology and seasonality modeling* (Vol. 8). Springer Science & Business Media.

Lloyd, J., & Taylor, J. A. (1994). On the Temperature Dependence of Soil Respiration. *Functional Ecology*, *8*(3), 315–323. https://doi.org/10.2307/2389824

Melaas, E. K., Richardson, A. D., Friedl, M. A., Dragoni, D., Gough, C. M., Herbst, M., Montagnani, L., & Moors, E. (2013). Using FLUXNET data to improve models of springtime vegetation activity onset in forest ecosystems. *Agricultural and Forest Meteorology*, *171*, 46–56.

Noormets, A. (2009). *Phenology of ecosystem processes: Applications in global change research*. Springer.

Oquist, G., & Huner, N. P. A. (2003). Photosynthesis of overwintering evergreen plants. *Annual Review of Plant Biology*, *54*, 329–355. https://doi.org/10.1146/annurev.arplant.54.072402.115741

Peaucelle, M., Janssens, I. A., Stocker, B. D., Descals Ferrando, A., Fu, Y. H., Molowny-Horas, R., Ciais, P., & Peñuelas, J. (2019). Spatial variance of spring phenology in temperate deciduous forests is constrained by background climatic conditions. *Nature Communications*, *10*(1), 5388. https://doi.org/10.1038/s41467-019-13365-1

Peñuelas, J., & Filella, I. (2001). Responses to a warming world. *Science*, *294*(5543), 793–795.

Peñuelas, J., Filella, I., Zhang, X., Llorens, L., Ogaya, R., Lloret, F., Comas, P., Estiarte, M., & Terradas, J. (2004). Complex spatiotemporal phenological shifts as a response to rainfall changes. *New Phytologist*, *161*(3), 837–846. https://doi.org/10.1111/j.1469-8137.2004.01003.x

Peñuelas, J., Rutishauser, T., & Filella, I. (2009). Phenology Feedbacks on Climate Change. *Science*, *324*(5929), 887–888. https://doi.org/10.1126/science.1173004

Repo, T., Leinonen, I., Ryyppö, A., & Finér, L. (2004). The effect of soil temperature on the bud phenology, chlorophyll fluorescence, carbohydrate content and cold hardiness of Norway spruce seedlings. *Physiologia Plantarum*, *121*(1), 93–100. https://doi.org/10.1111/j.0031-9317.2004.00307.x

Schwartz, M. D. (2003). *Phenology: An integrative environmental science*

Semenchuk, P. R., Gillespie, M. A. K., Rumpf, S. B., Baggesen, N., Elberling, B., & Cooper, E. J. (2016). High Arctic plant phenology is determined by snowmelt patterns but duration of phenological periods is fixed: An example of periodicity. *Environmental Research Letters*, *11*(12), 125006. https://doi.org/10.1088/1748-9326/11/12/125006

Starr, G., Oberbauer, S. F., & Ahlquist, L. E. (2008). The Photosynthetic Response of Alaskan Tundra Plants to Increased Season Length and Soil Warming. *Arctic, Antarctic, and Alpine Research*, *40*(1), 181–191. https://doi.org/10.1657/1523-0430(06-015)[STARR]2.0.CO;2

Tanja, S., Berninger, F., Vesala, T., Markkanen, T., Hari, P., Mäkelä, A., Ilvesniemi, H., Hänninen, H., Nikinmaa, E., Huttula, T., Laurila, T., Aurela, M., Grelle, A., Lindroth, A., Arneth, A., Shibistova, O., & Lloyd, J. (2003). Air temperature triggers the recovery of evergreen boreal forest photosynthesis in spring. *Global Change Biology*, *9*(10), 1410–1426. https://doi.org/10.1046/j.1365-2486.2003.00597.x

Walther, S., Voigt, M., Thum, T., Gonsamo, A., Zhang, Y., Köhler, P., Jung, M., Varlagin, A., & Guanter, L. (2016). Satellite chlorophyll fluorescence measurements reveal large-scale decoupling of photosynthesis and greenness dynamics in boreal evergreen forests. *Global Change Biology*, *22*(9), 2979–2996.

Wang, Y., Mao, Z., Bakker, M. R., Kim, J. H., Brancheriau, L., Buatois, B., Leclerc, R., Selli, L., Rey, H., Jourdan, C., & Stokes, A. (2018). Linking conifer root growth and production to soil temperature and carbon supply in temperate forests. *Plant and Soil*, *426*(1–2), 33–50. https://doi.org/10.1007/s11104-018-3596-7

Wheeler, J. a., Gonzalez, N. m., & Stinson, K. a. (2016). Red hot maples: Acer rubrum first-year phenology and growth responses to soil warming. *Canadian Journal of Forest Research*, *47*(2), 159–165. https://doi.org/10.1139/cjfr-2016-0288

Zhang, X., Friedl, M. A., Schaaf, C. B., Strahler, A. H., Hodges, J. C. F., Gao, F., Reed, B. C., & Huete, A. (2003). Monitoring vegetation phenology using MODIS. *Remote Sensing of Environment*, *84*(3), 471–475. https://doi.org/10.1016/S0034-4257(02)00135-9

Zohner, C. M., Benito, B. M., Svenning, J.-C., & Renner, S. S. (2016). Day length unlikely to constrain climate-driven shifts in leaf-out times of northern woody plants. *Nature Climate Change*, *6*(12), 1120–1123. https://doi.org/10.1038/nclimate3138

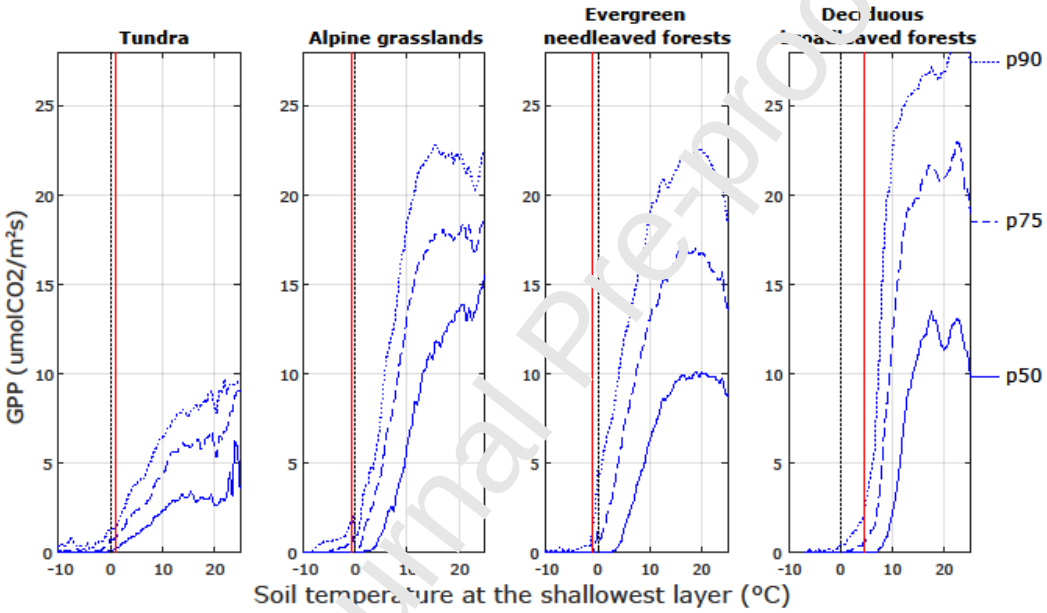

Figure 1 | Gross primary productivity (GPP) in relation to soil temperature in the FLUXNET sites. The x-axis shows soil temperature measured at the shallowest layer. The distribution of GPP is presented with the 50th percentile (continuous line), 75th percentile (dashed line), and 90th percentile (dotted line). The red line shows the lowest temperature in which GPP is significantly higher than 0°C. The temporal resolution of the GPP and temperature data is half-hourly.

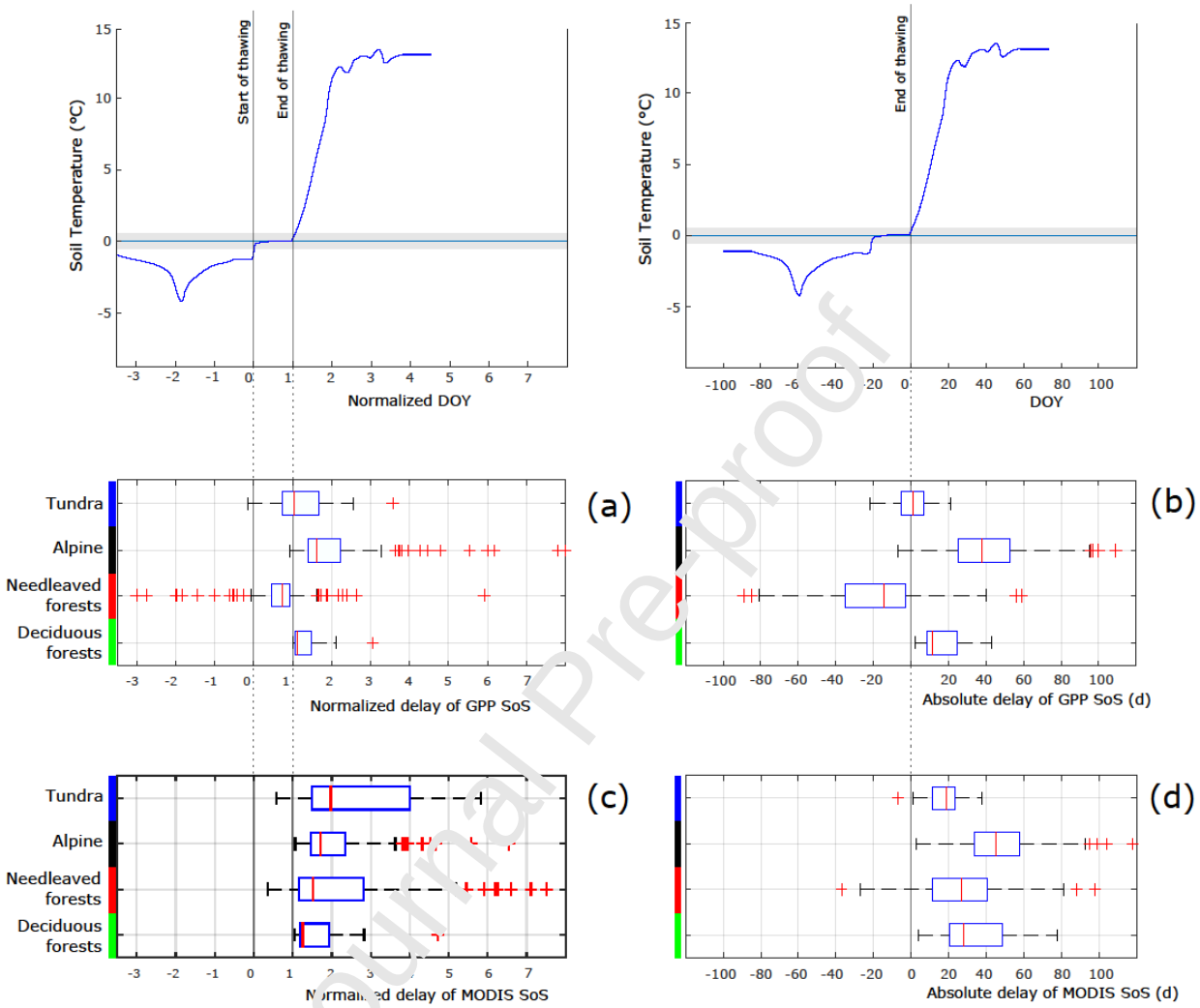

Figure 2 | Boxplots of the normalized delay (**(a)** and **(c)**) and absolute delay (**(b)** and **(d)**) of spring onset after the end of thawing (EoT) for tundra, alpine grasslands, needleaved forests, and deciduous forests. The absolute delay is the number of days between spring onset and EoT, and the normalized delay represents spring onset relative to thawing, with start of thawing (SoT) = 0 and EoT = 1. Spring onset is presented as FLUXNET gross primary productivity (GPP) start of season (SoS) in **(a)** and **(b)** and as MODIS SoS ('MidGreenup1' band in MCD12Q2v6 product) in **(c)** and **(d)**. The central mark of the boxplot indicates the median, the bottom and top edges indicate the 25th and 75th percentiles. The whiskers cover until the most extreme data points not considered outliers, and outliers are plotted with the '+' symbol.

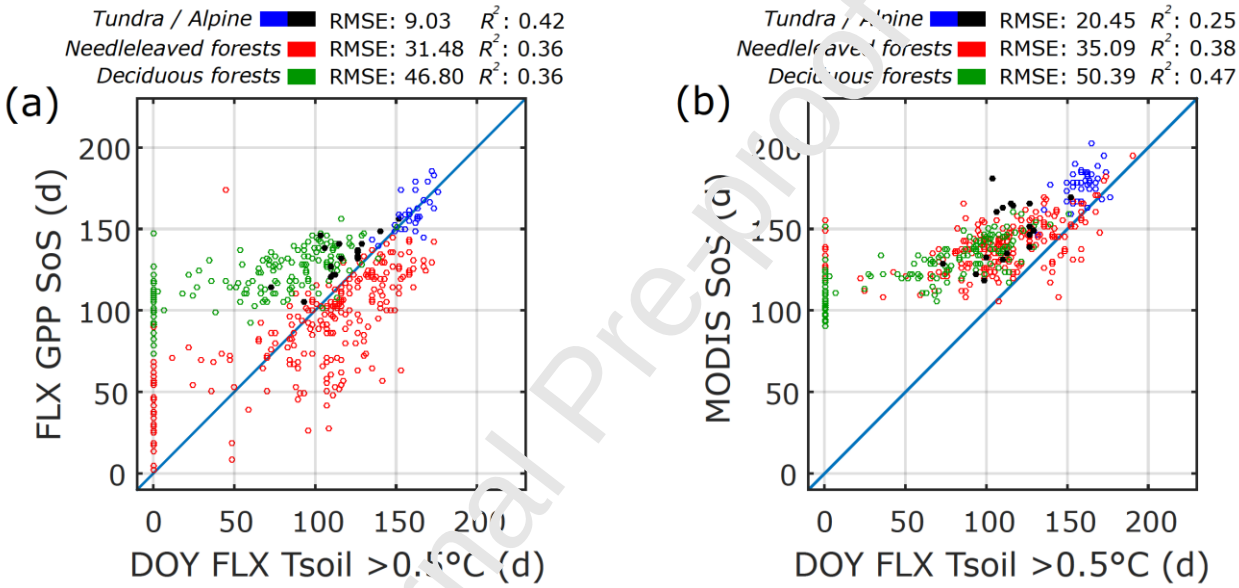

Figure 3 | Scatter plots of spring onset (gross primary productivity (GPP) start of season (SoS) **(a)** and MODIS SoS ('MidGreenup1' band in MCD12Q2v6 product) **(b)**) and the last day before the growing season using soil temperature >0.5 °C. Point colors represent tundra (blue), alpine grasslands (black), needleaved forests (red), and deciduous forests (green). Notice that the best fit between the spring onset and the end of thawing corresponds to tundra and alpine grasslands.

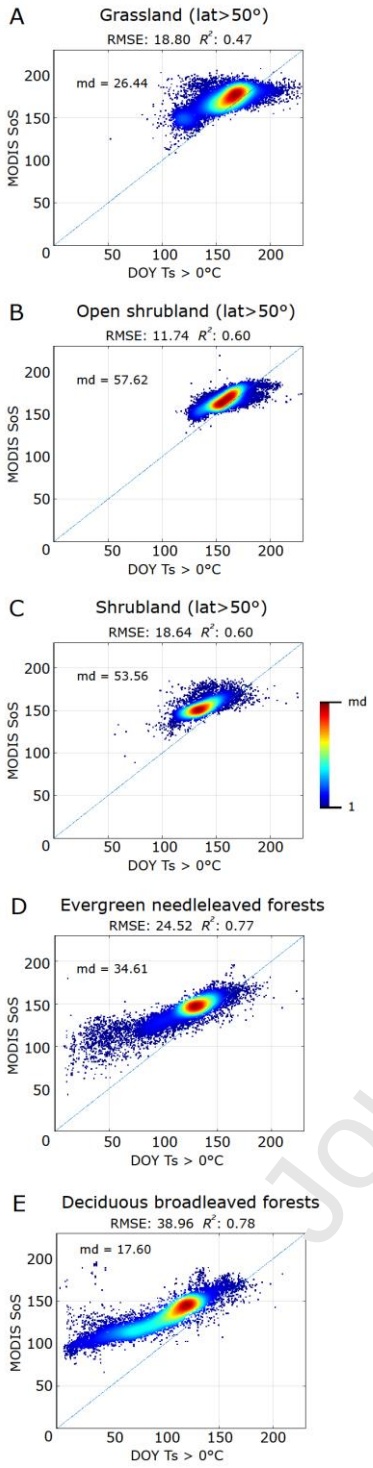

Figure 4 | Relationships between MODIS start of season (SoS) and end of thawing (EoT) estimated using the GLDAS dataset. Each panel represents MODIS SoS ('MidGreenup1' band in MCD12Q2v6 product) masked with the MODIS IGBP Land Cover product for cover types **(a)** grassland, **(b)** open shrubland, **(c)** shrubland, **(b)** evergreen needleleaved forests, and (**e**) deciduous broadleaved forests. The land cover types grassland, open shrubland, and shrubland for latitudes higher than 50° represent predominantly the tundra biome. The maximum density (md) varies depending on the land cover.

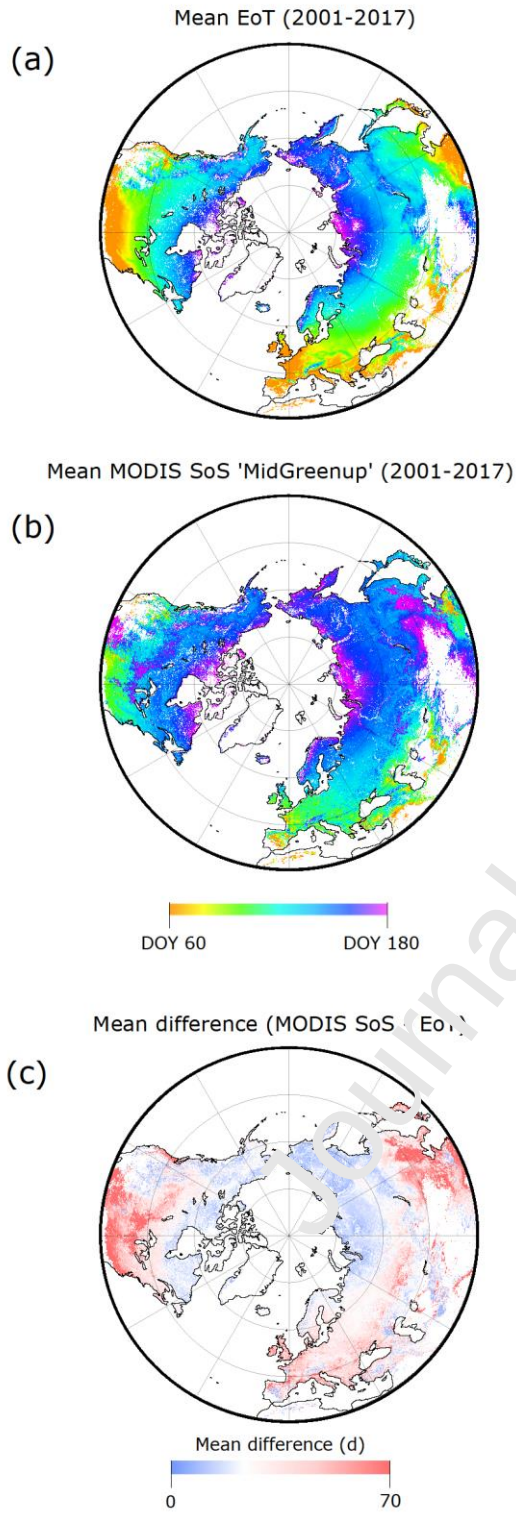

Figure 5 | Maps of **(a)** mean end of thawing (EoT), **(b)** mean MODIS start of season (SoS), and **(c)** mean difference (MODIS SoS - EoT) for the period 2001-2017. EoT was estimated using the GLDAS data set as the last day of the dormant period with soil temperatures <0.5 °C. MODIS SoS is the 'MidGreenup1' band in MCD12Q2v6 product. We resized MODIS SoS to the spatial resolution of the GLDAS dataset. The map projection is the Lambert Azimuthal Equal-Area.

Author contributions: AD and JP conceived the research idea. AD, AV, and JP designed the study. AD performed the analyses and wrote the first version of the manuscript. AD, AV, IF, DB, IJ, YF, SP, MP, PC, and JP contributed to the interpretation of the results and to revisions of the manuscript.

Declaration of interests

☒ The authors declare that they have no known competing financial interests or personal relationships that could have appeared to influence the work reported in this paper.

☐The authors declare the following financial interests/personal relationships which may be considered as potential competing interests:

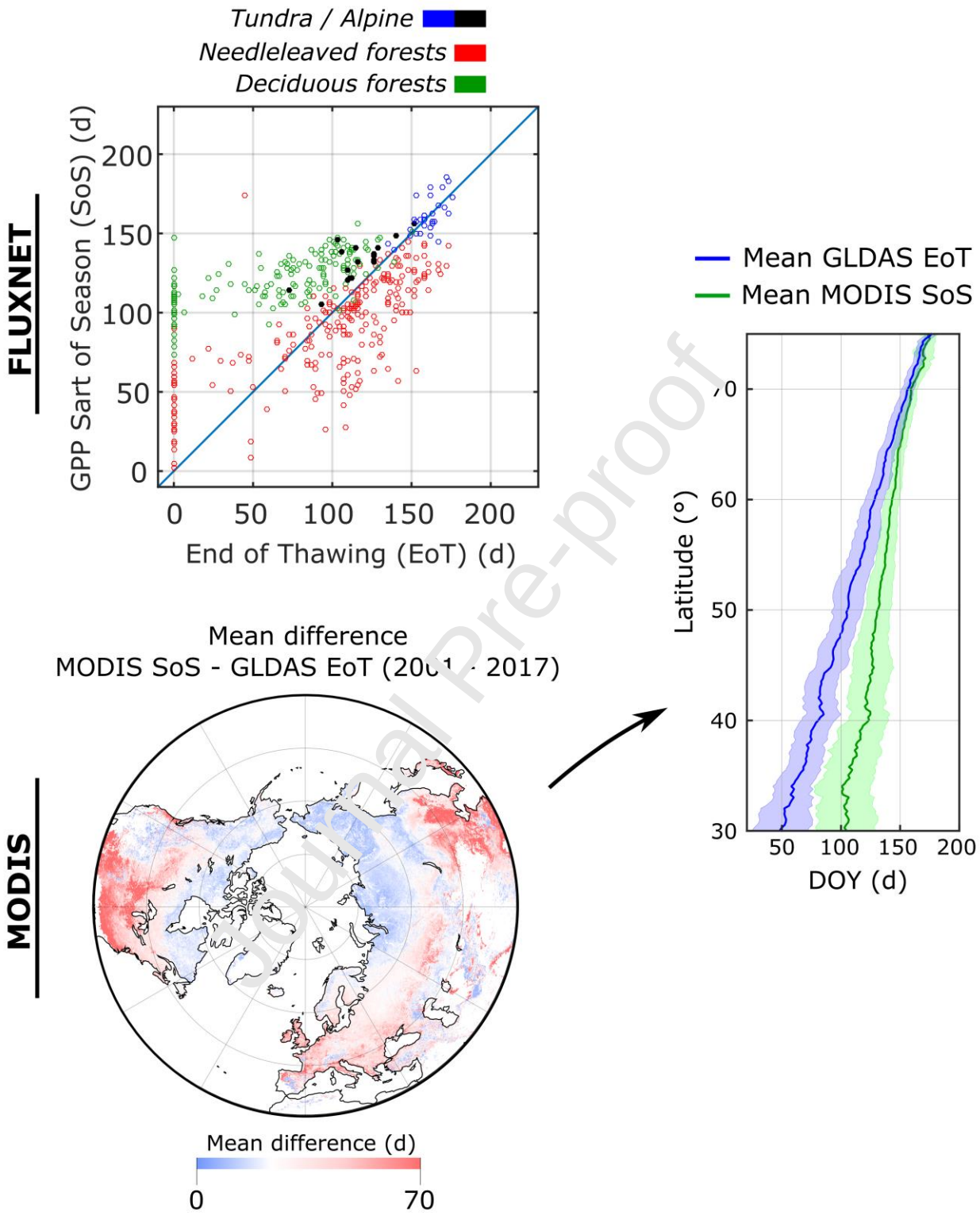

Highlights

- Vegetation may receive soil thawing as a signal to restore physiological activity.
- We estimated the delay between the soil thawing and the spring growth onset in 78 sites of the FLUXNET network and with remote sensing data.
- Soil thawing plays a role at the onset of spring growth in alpine biomes and at high latitudes, and the further north the vegetation grows the stronger is the role.

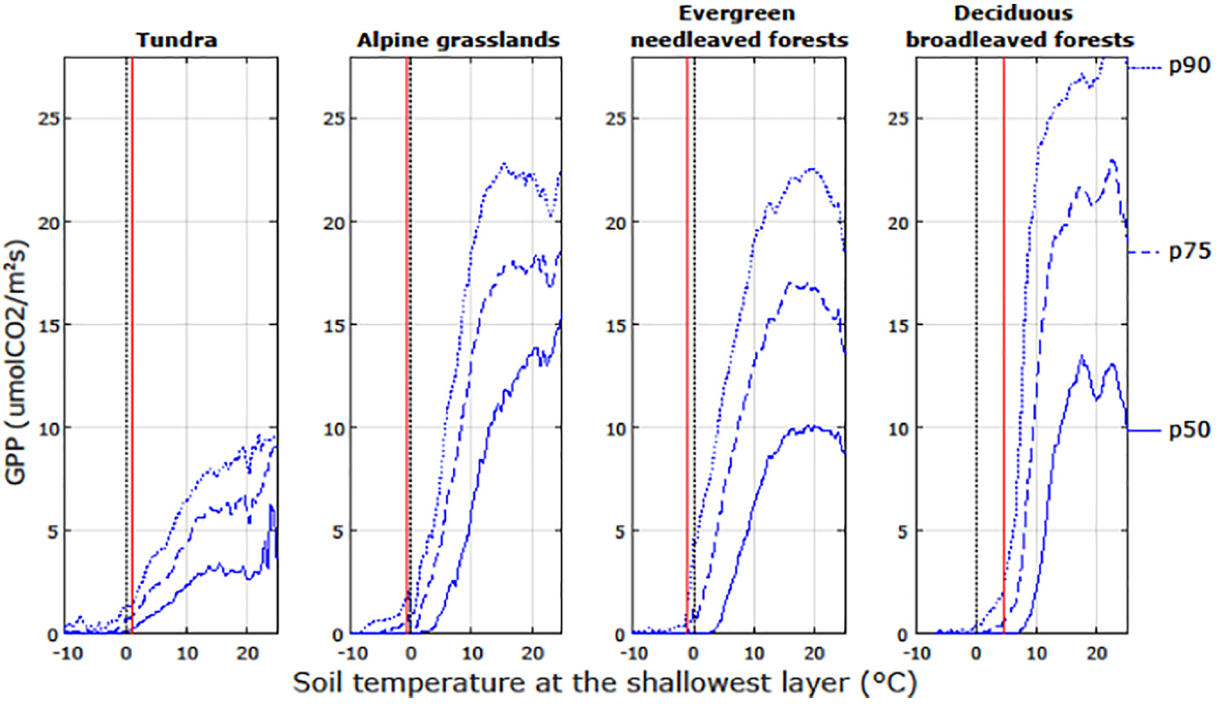
Tundra
Alpine grasslands
Evergreen needleaved forests
Deciduous broadleaved forests
p90
p75
p50
GPP (umolCO2/m²s)
Soil temperature at the shallowest layer (°C)

Figure 1

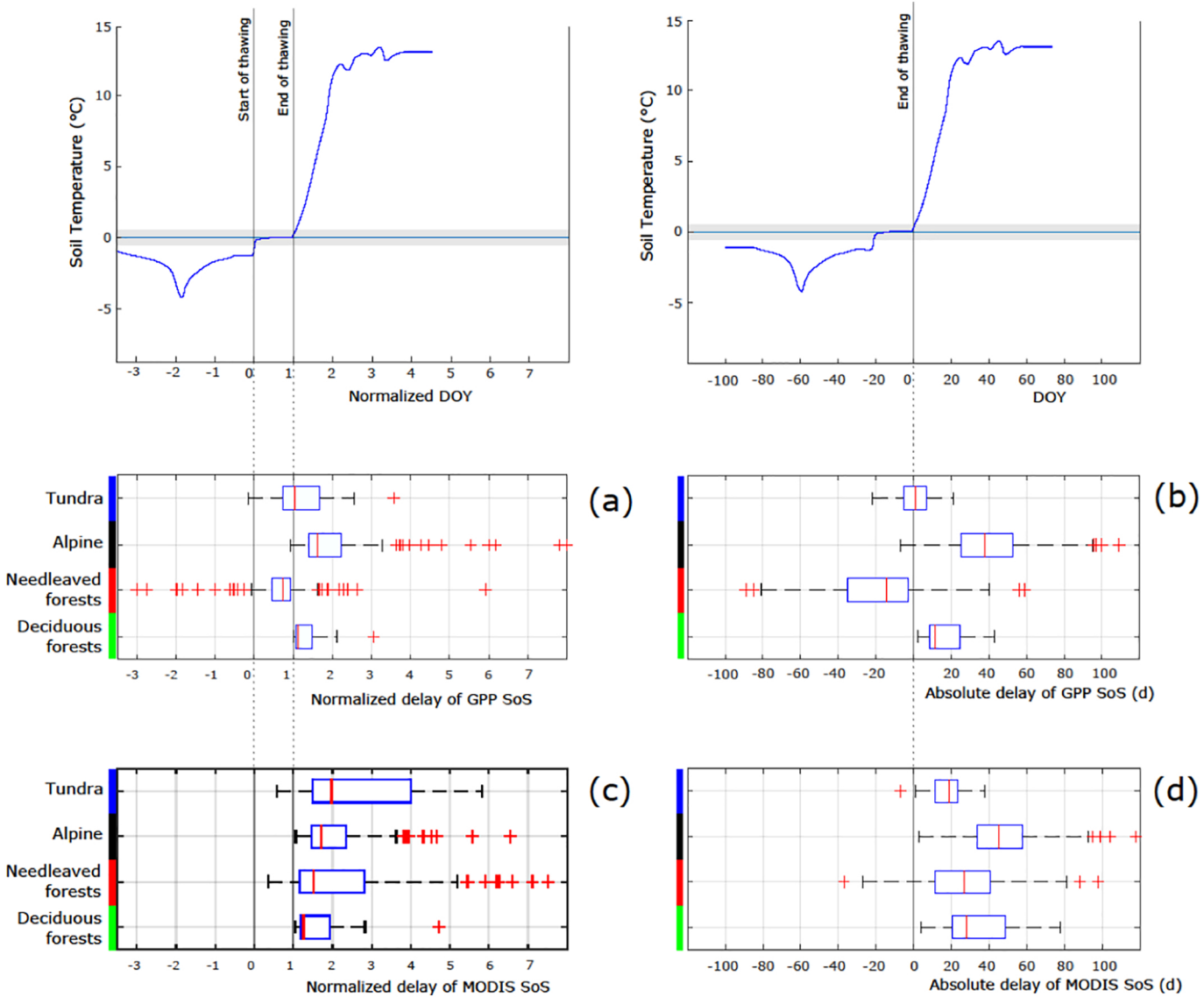
Soil Temperature (°C)
Start of thawing
End of thawing
Normalized DOY
DOY
Tundra
Alpine
Needleaved forests
Deciduous forests
(a)
(b)
(c)
(d)
Normalized delay of GPP SoS
Absolute delay of GPP SoS (d)
Normalized delay of MODIS SoS
Absolute delay of MODIS SoS (d)

Figure 2

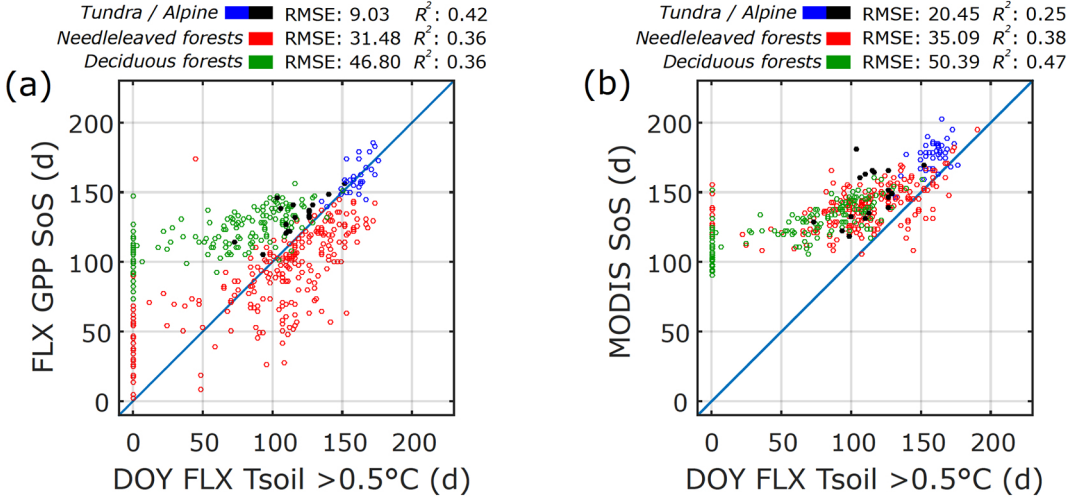
Tundra / Alpine RMSE: 9.03 R^2: 0.42
Needleleaved forests RMSE: 31.48 R^2: 0.36
Deciduous forests RMSE: 46.80 R^2: 0.36
(a)
FLX GPP SoS (d)
DOY FLX Tsoil >0.5°C (d)
Tundra / Alpine RMSE: 20.45 R^2: 0.25
Needleleaved forests RMSE: 35.09 R^2: 0.38
Deciduous forests RMSE: 50.39 R^2: 0.47
(b)
MODIS SoS (d)
DOY FLX Tsoil >0.5°C (d)

Figure 3

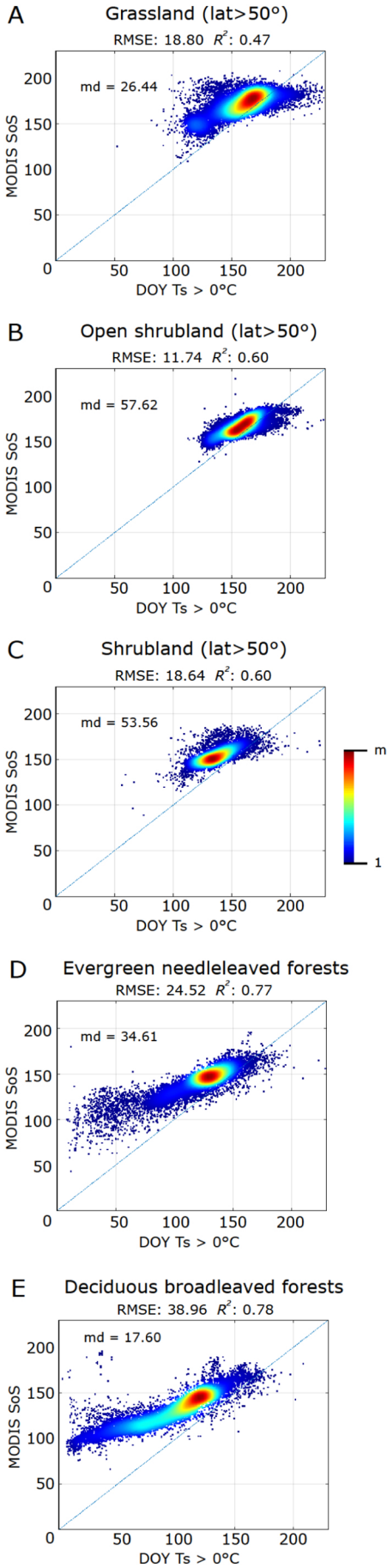
A
Grassland (lat>50°)
RMSE: 18.80 R^2: 0.47
md = 26.44
MODIS SoS
DOY Ts > 0°C
B
Open shrubland (lat>50°)
RMSE: 11.74 R^2: 0.60
md = 57.62
MODIS SoS
DOY Ts > 0°C
C
Shrubland (lat>50°)
RMSE: 18.64 R^2: 0.60
md = 53.56
MODIS SoS
DOY Ts > 0°C
md
1
D
Evergreen needleleaved forests
RMSE: 24.52 R^2: 0.77
md = 34.61
MODIS SoS
DOY Ts > 0°C
E
Deciduous broadleaved forests
RMSE: 38.96 R^2: 0.78
md = 17.60
MODIS SoS
DOY Ts > 0°C

Figure 4

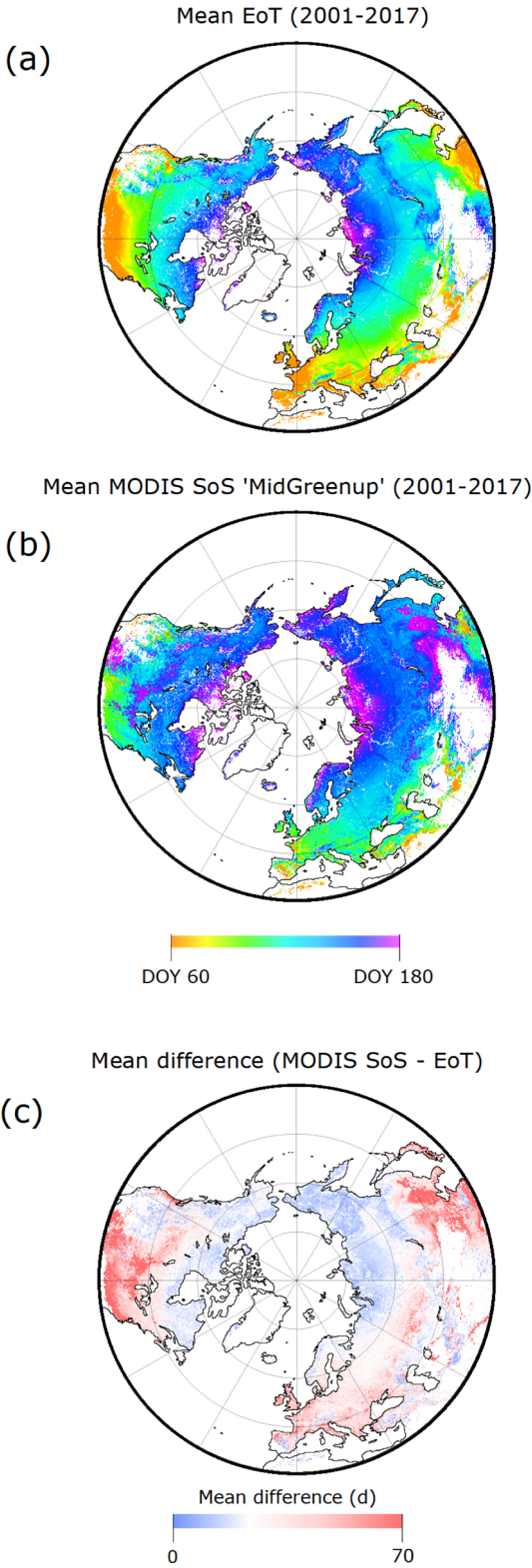
Mean EoT (2001-2017)
(a)
Mean MODIS SoS 'MidGreenup' (2001-2017)
(b)
DOY 60
DOY 180
Mean difference (MODIS SoS - EoT)
(c)
Mean difference (d)
0
70

Figure 5